



The papers that I have provided explains that electrospun-nanofibers face masks are a capable solution to provide sustainable filtration masks for re-use while keeping its efficacy and allowing for better breathability.

Currently N95 masks are being used by non-medical personal and these are in short supply, moreover these masks are meant for “one use only” yet non-medical people still re-use these.

The research we have provided clearly proves the following:

- Melt Blown Fiber (what N95 and “blue masks” are made of) are supposed to be used for “ONE-USE” and loses its efficacy in as little at 5 minutes. Nano fiber does not lose its efficacy.
- Melt Blown Fiber reduces its efficacy after 5 minutes (20%) and reduces to less than 65% within 24 hours making it impossible to re-use, even after 10 minutes where efficacy reduces to 80% (where NF stays at 90%).
- Nano Fiber DOES retain its efficacy after 24 hours up to 30 days!
- Our mask is actually 3 layers of Nanofiber that filter even aerosol level.

The conclusion by both papers is that Nano Fiber is a superior replacement for the current shortage of re-usable masks



## Electrospun Nanofibers-Based Face Masks

Mike Tebyetekerwa<sup>1</sup> · Zhen Xu<sup>2</sup> · Shengyuan Yang<sup>3</sup> · Seeram Ramakrishna<sup>4</sup>

Received: 25 May 2020 / Accepted: 10 June 2020 / Published online: 25 June 2020  
© Donghua University, Shanghai, China 2020

### Abstract

Textiles have proved to be very important materials to human beings since the time immemorial. And, fibers are the basic building units of these materials. In this perspective we substantiate the uniqueness and capability of nanofibers as active layers in face masks, to protect people against the novel coronavirus disease (COVID-19). This time-sensitive letter introduces the mechanisms based on which their active filters function, the uniqueness of electrospun nanofibers in face masks and do-it-yourself (DIY) steps to realize a fully functional face mask at home.

**Keywords** Electrospinning · Nanofibers · Face masks · COVID-19 · Textiles

### Introduction

Towards the end of December, 2019, an outbreak of a novel coronavirus disease (COVID-19) was reported in Wuhan, People's Republic of China [1]. As of 25 May 2020, the virus had spread to countries around the world and affected over 5.43 million people with more than 345,000 deaths reported [2]. To curb the rapid transmission of COVID-19,

various health organizations and responsible government ministries recommended people to use face masks to cover their nose and mouth when outside their homes. Moreover, the use of face mask is a standard safety procedure in some places and is a standard operating procedure for some workers, such as those in healthcare. The commonly used masks are the face (surgical) masks and respirator masks-P2 and N95 (Fig. 1a)[3]. Respirator masks are specially designed for high-risk medical settings and have the capability to protect the wearer from viruses and bacteria, whereas, surgical masks are designed for light medical settings and do not necessarily protect the wearer from bacteria and viruses. According to the world health organization, we quote that “Wearing a medical mask can limit the spread of certain respiratory viral diseases, including COVID-19. However, the use of a mask alone is not sufficient to provide an adequate level of protection. Other measures such as physical distancing and hand hygiene should be adopted” [4]. This makes it clear that a surgical mask alone cannot protect one from COVID-19 but can play some role in one's protection. This renders them important in the fight against COVID-19.

- ✉ Mike Tebyetekerwa  
mike.tebyetekerwa@anu.edu.au
- ✉ Zhen Xu  
z.xu19@imperial.ac.uk
- ✉ Shengyuan Yang  
cmseysy@dhu.edu.cn
- ✉ Seeram Ramakrishna  
seeram@nus.edu.sg

<sup>1</sup> Research School of Electrical, Energy and Materials Engineering, College of Engineering and Computer Science, The Australian National University, Canberra, ACT 2601, Australia

<sup>2</sup> Department of Chemical Engineering, Imperial College London, London SW7 2AZ, UK

<sup>3</sup> State Key Laboratory for Modification of Chemical Fibers and Polymer Materials, Shanghai “Belt & Road” International Joint Laboratory for Advanced Fiber and Low-Dimension Materials, College of Materials Science and Engineering, Donghua University, Shanghai 201620, People's Republic of China

<sup>4</sup> Centre for Nanofibers and Nanotechnology, National University of Singapore, Singapore 117581, Singapore

### How Face Masks Work?

Face masks are made up of fine microscopic sieves which are the active layers driving the mask's working mechanism. The fine microscopic sieve is made up of entangled mats of very fine fibers capable of creating convoluted pathways that the air along with any particle or viruses and bacteria

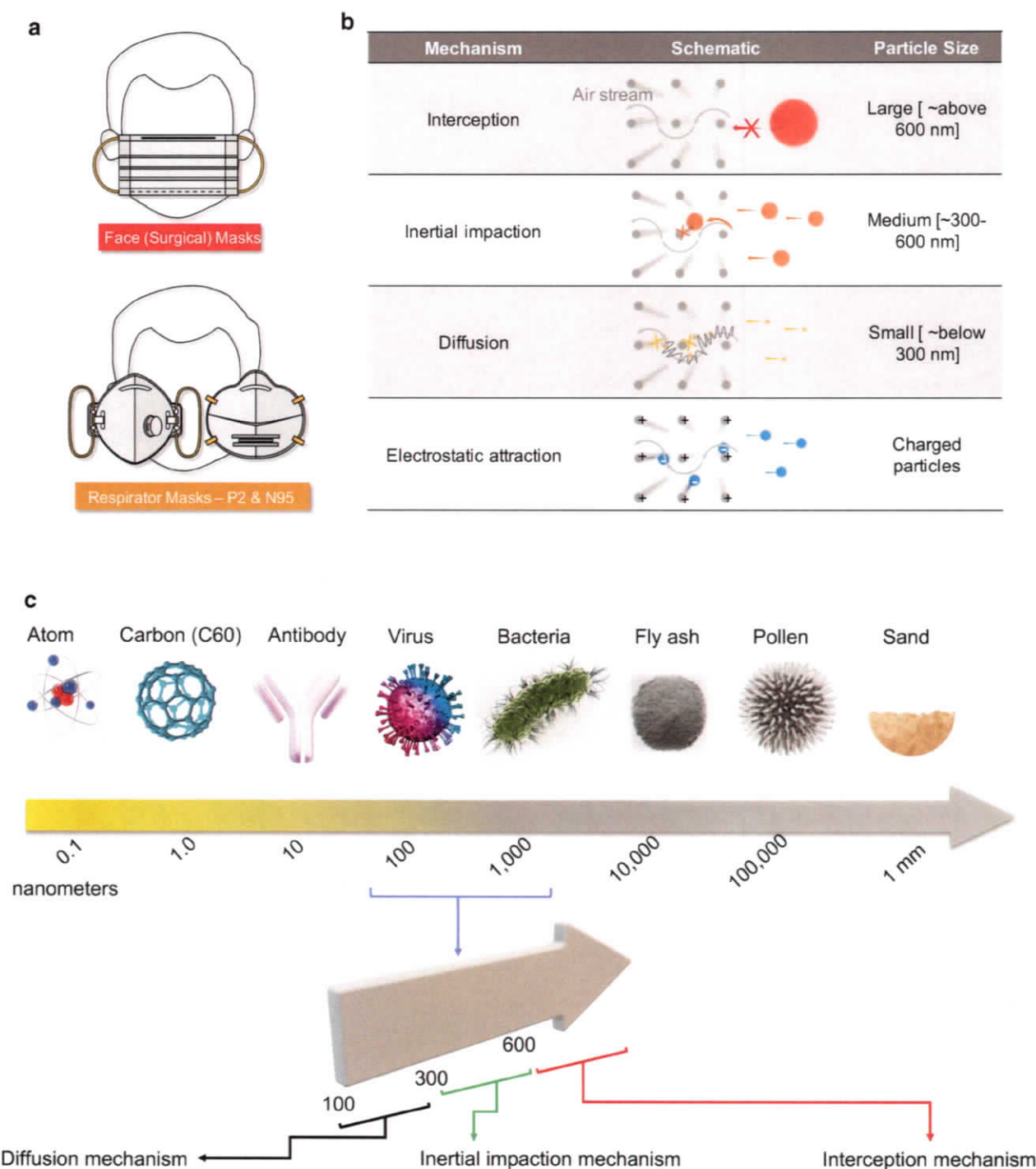


**Fig. 1** **a** Common types of protective masks. **b** Mechanisms of performance of face masks. **c** Basic concept of size on length scale of various particles in nature and the mechanism associated with mask filters when filtering them

one inhales has to take when in use. When the face mask is in use, three different types of particles can be blocked from reaching the wearer in four separate mechanisms (Fig. 1b). These particles are separately classified in three sizes, macro, micro, and nano (Fig. 1c). Charged particles have

also been added to the three particle types. Bigger macro-particles (above 600 nm) usually with sizes above the pore sizes of the mats cannot be permitted through the filters and are immediately blocked outside the masks in a mechanism called the interception mechanism. For micro fine particles,

(~300–600 nm) these can possibly move through the mat pores of the mask sieve, but there is higher probability for them to crash (just like any object moving in a non-straight path at high velocities) on the fiber walls on their course through the fiber entanglements. This is highly dictated by the particles' mass and velocity, hence making the particle to never reach the wearer. This is called the impact/collision mechanism. For nano-sized particles (below 300 nm), due to their very small sizes, they can easily move through the pores without even colliding with the pore walls with the help of air but are easily bombarded by the air molecules around them. For such particles to be captured, diffusion-based capture mechanism is followed which only happens in finer fibers (in nanometer sizes) and branched nanofibers. Electrospun nanofibers in this case prove more efficient. However, there are particles just between micro and nano ranges in a tune of ~300 nm, they hardly respect the impact/collision mechanism and the diffusion-based capture mechanism, and thus prove hard to filter in many face masks. This, therefore, requires multiple layers of the mats to delay such particles and let them obey one of the mechanisms. The presence of multiple filtration layers creates new different engineering problem of breathability of the final product. It is therefore important for an engineer to address the two competing demands of air filterability and air breathability to meet the ideal performance of a face mask. Electrospun nanofibers provide the needed balance with right process control during electrospinning. The last mechanism is electrostatic driven filtration, where the filter is made up

of charged mats which are capable of attracting the oppositely charged particles as a means of them not reaching the wearer.

## Uniqueness of Electrospun Nanofibers

The porosity and surface area of the fibers in the face mask dictate their breathability and filterability. Thus, to overcome these two competing properties, one has to find ways to engineer and balance the pores in the active filtration layer as well as the surface area of the fibers making up the mat. With electrospinning (Fig. 2a), it is possible to control these two properties *in situ* during the preparation of the nanofibers. Porosity of the mats can be controlled by changing the spinning nozzles, polymer solutions and the collection geometry of the nanofibers, which rationally defines the resultant fiber diameters and their packing density [5]. Breathability of the filtration layer in the electrospun nanofibers can also be controlled *in situ* by controlling the fiber collection time, and collection geometry of the nanofibers during spinning which both dictate the final thickness of the mat and areal weight. The method of collection the nanofibers can result into random nonwoven mats, aligned or meshed structures (see examples in Fig. 2b). Each arrangement is known to provide special breathability factor.

Electrospun nanofibers exist as nonwoven mats welded together physically with their parent polymer joints. This

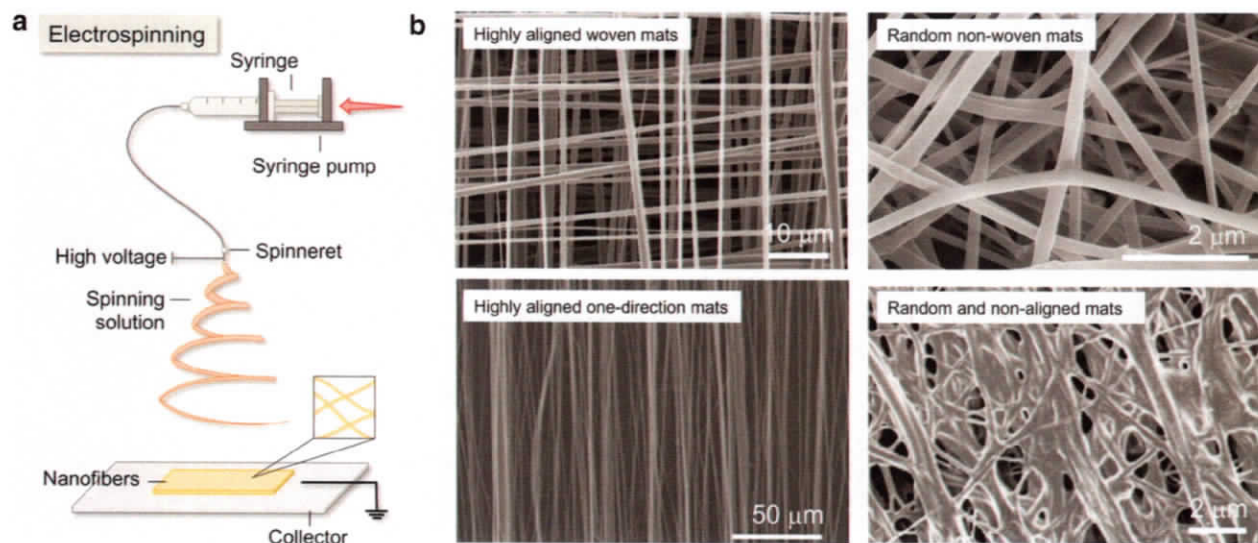


**Fig. 2** **a** Electrospinning technique. **b** Scanning electron microscope images of electrospun nanofibers collected on different geometries and styles. Highly aligned nanofibers (Adapted and reproduced from <https://www.nasa.gov/centers/langley/business/tg-img-fibermats.html>, accessed May 23, 2020). Highly aligned one-directional mats [6]. Reproduced with permission. Copyright 2017 Royal Society of

Chemistry. Random nonwoven mats [7]. Reproduced with permission. Copyright 2018 Royal Society of Chemistry. Random nonwoven mats. Random and non-aligned mats [8]. Adapted and reproduced with permission. Copyright 2019 WILEY-VCH Verlag GmbH & Co. KGaA, Weinheim

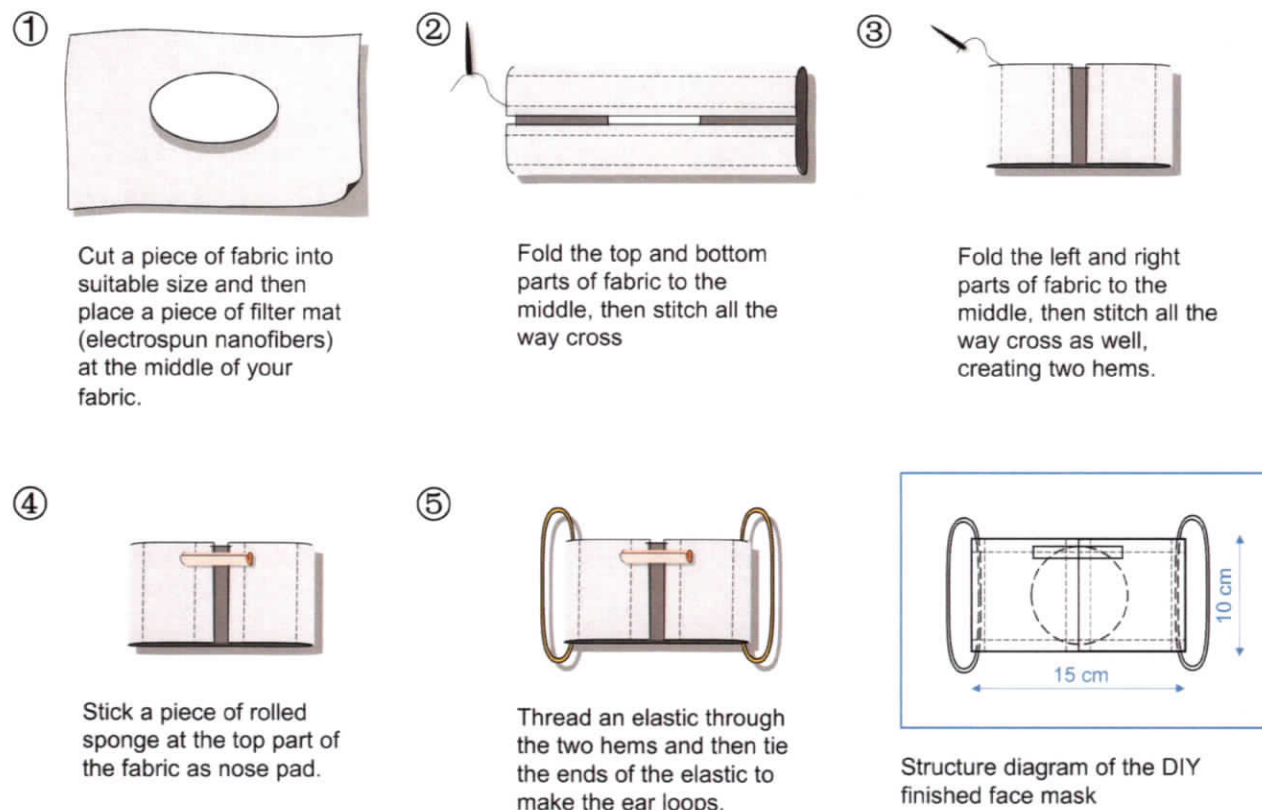


**Fig. 3** DIY steps of making a face mask at home

due to the fact that during the rapid electrospinning process in the high-field zone, the nanofibers continuously pile on each other when not perfectly dry, but in a wet state. Such a scenario makes the final nanofibers mats to have good physical interaction and durability during use. This is not the case in the common commercial face masks on market, whose active filter employs polypropylene (PP) fibers with small diameters in the range of ~500–1000 nm. The PP fibers filters achieves the three named filtration mechanisms with the fiber web kept together with the help of electrostatic charge responsible for keeping it in the required shape for maximum efficiency. Once the static charge is lost, their performance dramatically drops. Indeed, such filters lose static electricity when exposed to water and moisture, thus diminishing their filtering effect to almost half the original performance. Hence, the manufacturers recommend their disposal after a single use. Here, we propose to use electrospun non-woven fibers (with diameter below 100 nm) as filter. These fibers as explained are physically bundled and welded onto each other in a durable web, thus overcoming the limitation of static loss mechanism-based filters. Thus, even in presence of fluids and moisture (if hydrophobic), and with the same porosity, these filters can maintain the same breathability as conventional PP filters while sustaining filtration efficiency of more than 90%.

*PP  
Filter  
lose  
filtration*

To balance the two competing properties of breathability and filterability, therefore, electrospinning as a technique can be employed. With the right nozzle spinning gauges, collector geometry and polymer solution, it is possible to achieve balance between porosity and breathability of the mask filters at once in situ, thus making electrospinning technique favorable.

### Assembling Nanofibers-Based Face Mask At Home

A wide range of portable, safe, battery-operated, and easy-to-use electrospinners are available on the market which can be used to obtain the electrospun nanofiber mats with ease [9]. Then, after obtaining the right electrospun filter mats, they can be utilized when in a fully assembled working face mask. A do-it-yourself (DIY) approach to obtain a functional mask has been provided which can be followed at home (Fig. 3).

It is important to note that face mask should be made to conform to certain set standards. For example, breathability test MIL-M-36954 C: ΔP [10] -which quantifies the

face mask's resistance to airflow, fluid resistance test ASTM F1862 [11]- which determines the resistance of the face mask to fluid penetration, particulate filtration test ASTM F2299 [12]- which evaluates the filterability of the face mask, bacterial filtration test ASTM F2101 [13]- which determines the amount of bacteria larger than 3000 nm that can possibly be filtered by the mask, flammability test 16 CFR Part 1610: flame spread [14]- which measures the flame resistance properties of the mask. Beyond these, other important regular tests can be carried out which include; biocidal efficiency, viricidal efficiency, skin sensitivity, allergy, toxicity, etc.

## Summary

Until an effective vaccine is developed and made widely available, wearing protective face masks, maintaining personal hygiene and safe social distancing should be followed to prevent the spread of the COVID-19, and to provide a sense of security and well-being to everyone. This is leading to a worldwide surge in the use of billions of face masks every day-causing high demand for materials making them. In this work we have proposed the use of durable and yet reliable electrospun nonwoven filters with very small-fiber diameters (below 100 nm). The filter can be processed by suitable disinfection methods and protocols to achieve reuse (increased usage time) without compromising the filtration efficiency. Beyond these, future face masks need to be anti-viral as well as viricidal. The current electrospinning technology is mature [15], making the proposed strategy relatively low-cost with mass production capacity.

**Acknowledgements** M.T. acknowledges scholarship support from the Australian Government Research Training Program (RTP). Z.X. acknowledges the support from the China Scholarship Council (CSC). The Shanghai "Belt & Road" International Joint Laboratory Program (18520750400) administrated by the Science and Technology Commission of Shanghai Municipality is also acknowledged for its support.

## Compliance with ethical standards

**Conflict of interest** There is no conflict of interest to declare.

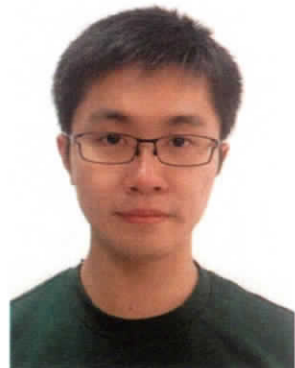
## References

- Wu F, Zhao S, Yu B, Chen Y-M, Wang W, Song Z-G, et al. A new coronavirus associated with human respiratory disease in China. *Nature*. 2020;579(7798):265–9.
- Coronavirus disease (COVID-2019) situation reports. World Health Organisation (WHO). 2020. <https://www.who.int/emergencies/diseases/novel-coronavirus-2019/situation-reports>. Accessed May 25, 2020.
- Types and uses of face masks. 2020. <https://www.safeworkaustralia.gov.au/doc/types-and-uses-face-masks>. Accessed May 25, 2020.
- Q&A: Masks and COVID-19. 2020. <https://www.who.int/emergencies/diseases/novel-coronavirus-2019/question-and-answers-hub/q-a-detail/q-a-on-covid-19-and-masks>. Accessed May 25, 2020.
- Soliman S, Sant S, Nichol JW, Khabiry M, Traversa E, Khademhosseini A. Controlling the porosity of fibrous scaffolds by modulating the fiber diameter and packing density. *J Biomed Mater Res A*. 2011;96(3):566–74. <https://doi.org/10.1002/jbm.a.33010>.
- Batnyam O, Suye S, Fujita S. Direct cryopreservation of adherent cells on an elastic nanofiber sheet featuring a low glass-transition temperature. *RSC Adv*. 2017;7(81):51264–71. <https://doi.org/10.1039/c7ra10604a>.
- Marriam I, Wang XP, Tebyetekerwa M, Chen GY, Zabihi F, Pionteck J, et al. A bottom-up approach to design wearable and stretchable smart fibers with organic vapor sensing behaviors and energy storage properties. *J Mater Chem A*. 2018;6(28):13633–43. <https://doi.org/10.1039/c8ta03262a>.
- Li H, Wu T, Xue J, Ke Q, Xia Y. Transforming nanofiber mats into hierarchical scaffolds with graded changes in porosity and/or nanofiber alignment. *Macromol Rapid Commun*. 2020;41(3):e1900579. <https://doi.org/10.1002/marc.201900579>.
- Portable Electrospinning. 2020. <https://electrospintech.com/portablespin.html#.XsvVgC2B1QJ>. Accessed May 25, 2020 2020.
- MIL-M-36954C. <https://www.frazierinstrument.com/refernce/standards/organizations/mil/abstract-mil-m-36954c.html> (Accessed May 25, 2020).
- ASTM F1862/F1862M-17, Standard test method for resistance of medical face masks to penetration by synthetic blood (Horizontal Projection of Fixed Volume at a Known Velocity), ASTM International, West Conshohocken, PA, 2017, [www.astm.org](http://www.astm.org). Accessed 25 May 2020.
- ASTM F2299 / F2299M-03(2017), Standard test method for determining the initial efficiency of materials used in medical face masks to penetration by particulates using latex spheres, ASTM International, West Conshohocken, PA, 2017, [www.astm.org](http://www.astm.org). Accessed 25 May 2020.
- ASTM F2101–19, Standard Test Method for Evaluating the Bacterial Filtration Efficiency (BFE) of Medical Face Mask Materials, Using a Biological Aerosol of *Staphylococcus aureus*, ASTM International, West Conshohocken, PA, 2019, [www.astm.org](http://www.astm.org). Accessed 25 May 2020.
- 6 CFR Part 1610. Code of Federal Regulations, Title 16, Chapter II, Consumer Product Safety Commission. *Federal Register* 2007: 603–620. 16 CFR Part 1610. Standard for the flammability of clothing textiles, proposedrules. *Federal Register*. 2007;72(38):8844–8868
- Tebyetekerwa M, Ramakrishna S. What Is Next for Electrospinning? *Matter*. 2020;2(2):279–83. <https://doi.org/10.1016/j.matt.2020.01.004>.



**Mike Tebyetekerwa** obtained his Masters in Materials Science and Engineering from Donghua University, Shanghai-China, in 2018 with his thesis focusing on functional fibrous materials under the co-supervision of Prof. Meifang Zhu and Dr Shengyuan Yang. He is currently a PhD candidate at the Australian National University, Canberra, with a focus on semiconducting 2D materials for use in future photovoltaics. His work focuses much on utilizing photoluminescence spectroscopy

to understand these materials and their devices (including; silicon, perovskites, similar emerging and fluorescent polymer materials). He still carries out active research with regards to functional fibrous materials for energy and environment applications.



**Zhen Xu** received his Undergraduate degree (honours) in Polymer Materials and Engineering from Donghua University in 2017. His undergraduate research focused on electrospun Polyindole nanofibers for all-solid-state flexible supercapacitors under the supervision of Dr. Shengyuan Yang. He is currently a PhD candidate in Chemical Engineering at the Imperial College London, focusing on nature-inspired hierarchical carbon materials for next-generation sodium batteries.



**Dr Shengyuan Yang** obtained his bachelor's degree from Fudan University in 2008. Then, he pursued his doctorate at the National University of Singapore under the supervision of Prof. Seeram Ramakrishna after receiving the prestigious NGS scholarship, which was completed in 2013. Finally, he returned home and joined the College of Materials Sciences and Engineering, Donghua University (DHU), in late 2014 as an associate professor. His research is centered on the novel applications of functional electrospun nanomaterials for wearable electronics and smart clothes. He is actively participating in several key national

and state R&D projects. He is also currently the vice director of the DHU International Cooperation Office.



**Academian Everest Chair Seeram Ramakrishna, FREng** is a Professor at the National University of Singapore (NUS) at the center for nanofibers and nanotechnology. He received his PhD from the University of Cambridge, UK. He is an elected Fellow of UK Royal Academy of Engineering (FREng); Singapore Academy of Engineering; Indian National Academy of Engineering; and ASEAN Academy of Engineering & Technology; American Association of the Advancement of Science

(AAAS) and many others. Thomson Reuters identified him among the World's Most Influential Scientific Minds. His Google Scholar H-index exceeds 150 and his publications have attracted over 100,000 citations Clarivate Analytics recognized him among the Top 1% Highly Cited Researchers in the world in materials science and crossfields categories. Microsoft Academic ranked him among the top 36 salient authors out of three million materials researchers worldwide. He innovatively utilizes electrospun nanofibers in various applications.



## Reusability Comparison of Melt-Blown vs Nanofiber Face Mask Filters for Use in the Coronavirus Pandemic

Sana Ullah,<sup>II</sup> Azeem Ullah,<sup>II</sup> Jaeyun Lee,<sup>II</sup> Yeonsu Jeong,<sup>II</sup> Motahira Hashmi, Chunhong Zhu, Kye Il Joo, Hyung Joon Cha,\* and Ick Soo Kim\*



Cite This: *ACS Appl. Nano Mater.* 2020, 3, 7231–7241



Read Online

ACCESS |

Metrics & More

Article Recommendations

Supporting Information

**ABSTRACT:** Shortage of face masks is a current critical concern since the emergence of coronavirus-2 or SARS-CoV-2 (COVID-19). In this work, we compared the melt-blown (MB) filter, which is commonly used for the N95 face mask, with nanofiber (NF) filter, which is gradually used as an effective mask filter, to evaluate their reusability. Extensive characterizations were performed repeatedly to evaluate some performance parameters, which include filtration efficiency, airflow rate, and surface and morphological properties, after two types of cleaning treatments. In the first cleaning type, samples were dipped in 75% ethanol for a predetermined duration. In the second cleaning type, 75% ethanol was sprayed on samples. It was found that filtration efficiency of MB filter was significantly dropped after treatment with ethanol, while the NF filter exhibited consistent high filtration efficiency regardless of cleaning types. In addition, the NF filter showed better cytocompatibility than the MB filter, demonstrating its harmlessness on the human body. Regardless of ethanol treatments, surfaces of both filter types maintained hydrophobicity, which can sufficiently prevent wetting by moisture and saliva splash to prohibit not only pathogen transmission but also bacterial growth inside. On the basis of these comparative evaluations, the wider use of the NF filter for face mask applications is highly recommended, and it can be reused multiple times with robust filtration efficiency. It would be greatly helpful to solve the current shortage issue of face masks and significantly improve safety for front line fighters against coronavirus disease.

**KEYWORDS:** coronavirus, face mask, nanofiber filter, melt blown filter, reusability, cell study, filtering efficiency

### INTRODUCTION

Since the emergence of the new type of coronavirus (COVID-19 hereafter), the number of infected persons is increasing exponentially. According to the World Health Organization (WHO), 6 663 304 cases of COVID-19 have been reported as of June 6, 2020.<sup>1</sup> There are limited data on clinical characteristics of COVID-19; some of the researchers claimed a 4.3% mortality rate while others claimed less.<sup>2,3</sup> Some of the major symptoms and parameters have been reported to investigate the presence of COVID-19 in a patient.<sup>4</sup> Since the first infection reported in early December 2019, there have been extensive studies about the origin, symptoms, trend of infection, the transmission of infection from person to person, possible preparation of vaccine (which has not yet prepared successfully by any of the researchers), and precautionary measures.<sup>5–14</sup> Some researchers claimed that coronavirus can be inactivated by heat using the N95 face mask, which is known to be one of best face masks but is limited to one-time use only.<sup>5</sup>

Personal protective equipment (PPE) became a hot issue since the emergence of COVID-19 pandemic. Because there is

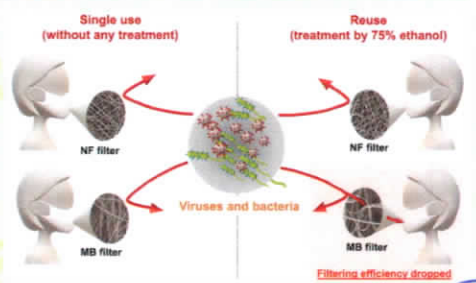
no possible vaccine at this time, PPE is a major concern in fighting against this pandemic. Even higher authorities and institutions including WHO are concerned about the shortage of face masks, suggesting the public use of cloth masks even if medical masks are not available in markets. China is a major producer of face masks with almost 50% contribution in global face masks consumption.<sup>15</sup> However, it is clear that COVID-19 has badly affected the production and supply of face masks throughout the world. Countries having the capacity of producing face masks are also suffering from a shortage of face masks. These countries include developed nations like the European Union, U.S.A., Japan, and the U.K. N95 is one of the best available filters so far, but it is limited to single-use only. It was reported that COVID-19 can survive for a week on the

Received: June 6, 2020  
Accepted: June 12, 2020  
Published: June 12, 2020



<https://dx.doi.org/10.1021/acsnano.0c01562>

7231



Wider  
use  
of  
Application)

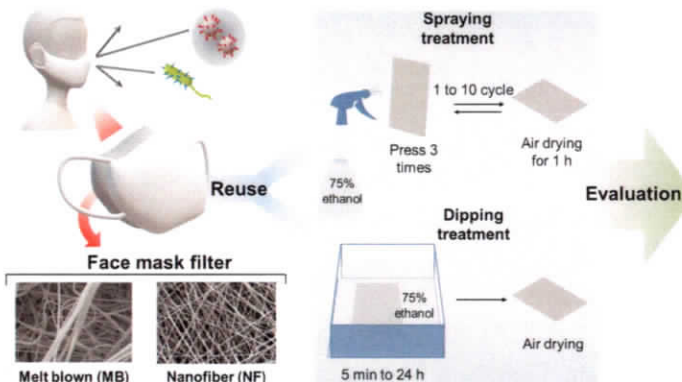


**Figure 1.** Schematic diagram on spraying and dipping treatments of face mask filters using 75% ethanol for evaluation of reusability.

outer surface of the face mask. That makes it complementary to proper treatment before reuse or even for disposal of face masks. However, current studies have been done to sterilize N95 filter-based face masks using UV light.<sup>16</sup> In general, the N95 filter is produced by a melt-blown (MB) process. Studies also show that common fabrics may have filtering efficiency of 80–95% depending on fabric structures.<sup>17–19</sup>

It was reported about the investigation on the effect of nanotreatment (treatment by nanofunctional materials such as nanoparticles) on the N95 and surgical masks subjected to thermophysiological responses and discomfort.<sup>20</sup> They reported that subjects wearing nanotreated surgical masks have significantly lower heart rates. The outer surface temperature of the nanotreated surgical masks was higher than that of the N95 masks. However, microenvironment and skin temperatures were lower in the nanotreated surgical masks. Furthermore, N95 masks reported having significantly higher absolute humidity inside the mask surface. All nanotreated surgical masks were reported to have a significantly lower perception of heat, humidity, and overall discomfort.<sup>20</sup> There was a study on the protective performance of N95 and surgical face masks. They reported that N95 masks had significantly lower air permeability and water vapor permeability than surgical masks. *In vivo* test revealed that N95 masks can filter out 97% of the foreign bodies, while surgical masks can be as good as up to 95%. Nanotreated surgical masks can provide additional protective functions in stopping capillary diffusion and antibacterial activities.<sup>21</sup> The study was basically conducted to investigate N95 protection against the airborne viruses versus surgical masks.<sup>22</sup> They reported that N95 filtering masks may not provide the expected protection level against significantly small particles but are much more efficient than the surgical masks against the infection causing agents in the range of 10–80 nm. There was a survey on the risks involved in causing headaches due to wearing N95 respirators.<sup>23</sup> They reported that higher humidity levels, breath resistance, and accumulation of heat inside the microclimate of the masks result in headaches. Thus, they suggested shorter duration of mask wearing can significantly reduce the severity of the headaches. A survey was also conducted on the protection level of the surgical masks versus N95 masks for preventing influenza among the health care workers.<sup>24</sup> They

reported that N95 masks were not better in protection against influenza than the surgical masks.

Electrospun nanofibers have a wide range of applications in healthcare,<sup>25–31,36</sup> environmental engineering,<sup>31,32</sup> and energy storage sectors.<sup>33</sup> Currently, nanofibers are being produced in bulk quantity in some countries including Korea, Japan, the U.S.A., and European countries. Nanofibers are the best replacement for microfibers and thin films due to their distinct features including the higher surface area which can be functionalized for desired the property, uniform morphology, consistency in structural properties, and simple technique to fabricate nanofibrous mats. Thus, nanofiber filters are gradually used for mask applications in the world. In the present work, we performed a comparative study on the performance properties of MB (N95) and nanofiber-based air filter masks for evaluation on reusability after cleaning (spraying and dipping) using 75% ethanol by determinations of air permeability, surface area, porosity, morphological properties, and filter performance (Figure 1).

## RESULTS AND DISCUSSION

**Physicochemical Study.** FTIR spectra of the MB and NF filters are shown in Figure 2. The FTIR spectrum of the MB filter confirms the polypropylene composition of the MB filter, and the peak at 2922 cm<sup>-1</sup> represented the CH<sub>2</sub> group vibration in main PP polymer chain. The spectrum also showed four peaks in the wavelength range of 3000–2800 cm<sup>-1</sup>; the peaks at 2955 and 2873 cm<sup>-1</sup> can be attributed to CH<sub>3</sub> asymmetric and symmetric stretching vibrations, while the peaks at 2922 and 2843 cm<sup>-1</sup> were due to CH<sub>2</sub> symmetric and asymmetric vibrations, respectively.<sup>34</sup> The intense peaks at 1478 and 1360 cm<sup>-1</sup> were caused by the CH<sub>2</sub> scissor vibrations or CH<sub>3</sub> symmetric and asymmetric deformation vibrations. PP FTIR spectrum showed characteristic fingerprint peaks in the region of 1200–750 cm<sup>-1</sup>. These peaks can be attributed to C–C as symmetric stretching, CH<sub>3</sub> asymmetric rocking, and C–H wagging vibrations and CH<sub>2</sub> rocking vibrations.<sup>34,35</sup> In the spectra of the NF filter, the FTIR spectrum of spun bond PET side showed an intense peak 1704 cm<sup>-1</sup> which is a characteristic of C=O symmetric stretching, and also the stretching can be seen at 1257 cm<sup>-1</sup>. The moderate C–H stretching can be seen at 2947 cm<sup>-1</sup>. A very weak peak at 3437

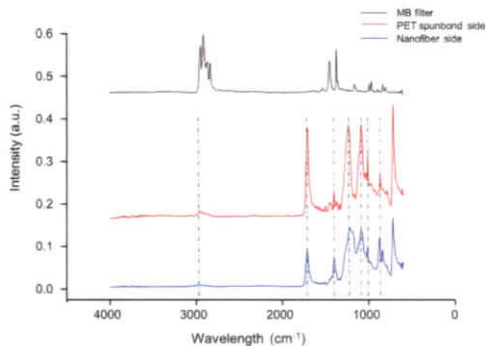


**Figure 2.** FTIR-ATR spectra of MB filter and NF filter (both sides; nanofiber and spun bond sides). FTIR spectra confirm the polypropylene composition of the MB filter, while they confirm PET and PVDF composition in the NF filter.

$\text{cm}^{-1}$  was attributed to the  $-\text{OH}$  group bonded to  $\text{C}=\text{O}$ . The peak at  $983 \text{ cm}^{-1}$  can be attributed to the out of plane bending of the  $-\text{OH}$  group in PET chains. The peaks observed at  $1250\text{--}950 \text{ cm}^{-1}$  are assigned to C–C stretching and C–H in plane bending in the PET polymer chain.<sup>36</sup> The peaks at  $1431 \text{ cm}^{-1}$  can be attributed to C–H deformation in the PVDF polymer chain.<sup>37</sup> The peak at  $869 \text{ cm}^{-1}$  was attributed to  $\alpha$  crystal of the PVDF.<sup>38</sup> The peak at  $1177 \text{ cm}^{-1}$  was attributed to the C–F stretching.<sup>39</sup>

**Evaluation of Filter Performance.** To evaluate reusability of MB and NF face mask filters, we used two types of cleaning procedures including 75% ethanol spraying up to 10 cycles (1 cycle is 3 times press of sprayer) and dipping in 75% ethanol. All possible parameters were considered for comparative characterizing the performance of MB and NF filters before and after cleaning with ethanol. First, air permeability (air flow rate) of both filters was measured (Figure 3a). It was observed that air permeability (in cfm unit) of MB filter was recorded  $\sim 27.2$  cfm as an average value before ethanol treatment. However, there was not a significant difference noted after ethanol treatment regardless of cleaning types. In the case of the NF filter, air permeability was about

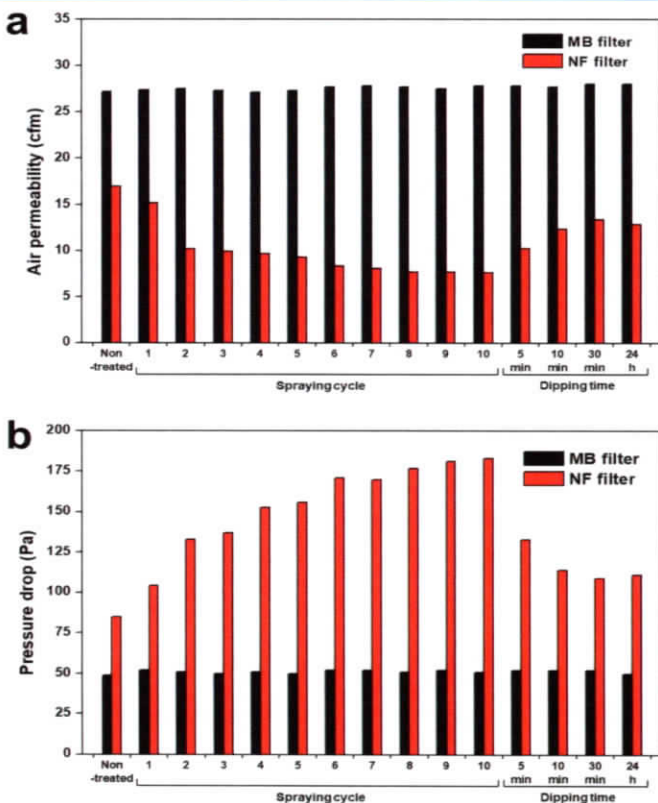


**Figure 3.** (a) Air permeability and (b) pressure drop for MB and NF face mask filters before and after spraying and dipping treatments using 75% ethanol.

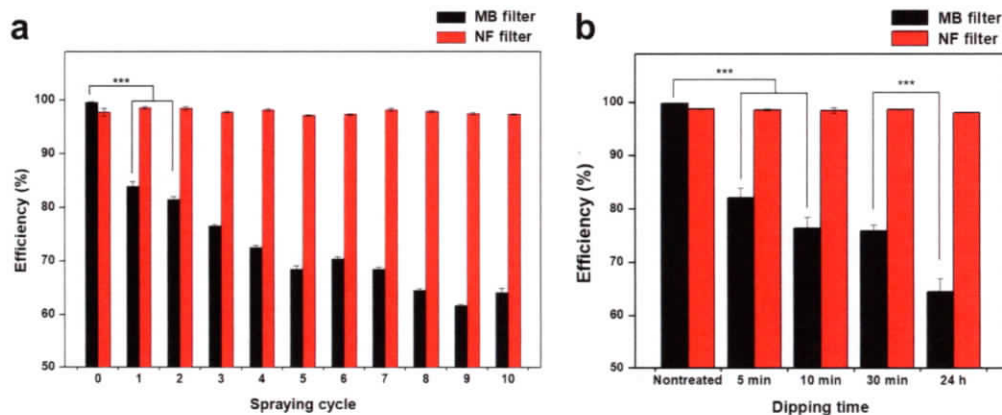


**Figure 4.** Filtration efficiency of MB and NF face mask filters according to (a) cycle numbers in spraying treatment and (b) time of dipping treatment. The values and error bars represent the mean  $\pm$  standard deviations of at least three samples with statistical significance from Student's unpaired *t* test (\*\**p* < 0.005).

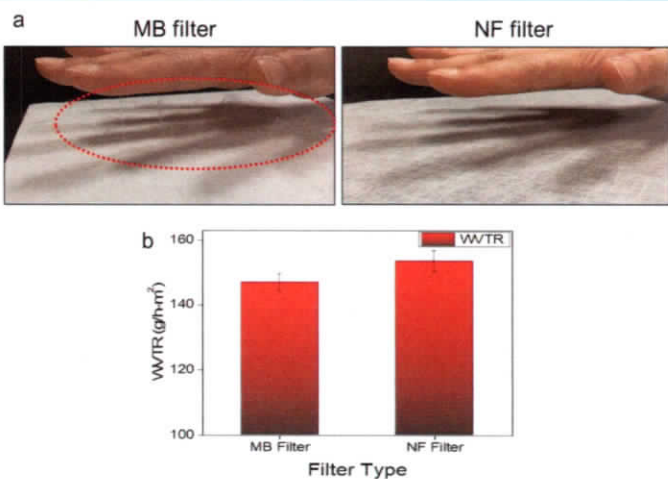


**Figure 5.** (a) Observation of static charge on the surfaces of MB and NF face mask filters and (b) water vapor transport rate of MB and NF filters.

17.0 cfm before cleaning but slightly decreased after ethanol treatment. Because the PVDF-based NF filter in this work was supported by spun-bond polyethylene terephthalate (PET), it may be one of the possibilities that when the NF filter was treated with ethanol, PET could be depolymerized to diethylene or monoethylene. While 100% depolymerization of PET is only possible in supercritical conditions, partial depolymerization is possible.<sup>40,41</sup> Thus, partial depolymerization of PET might make NF filter flatter rather than round, decreasing pore size through changing of the morphology of spun-bond PET. Thus, it can be concluded MB filter does not have a significant effect on air permeation by ethanol treatment; however, the NF filter exhibited slightly lower air permeability after ethanol treatment.

Next, the pressure drop was investigated to analyze inhaling/exhaling difficulties which are dependent on porous structure,

morphology, and construction of each filter. It was observed that the pressure drop for the MB case was lower than the NF filter (Figure 3b). In the case of the MB filter, there was no significant pressure drop when treated with ethanol. However, while the pressure drop of the NF filter was increased when treated with ethanol, it was within limits of safe use.<sup>42</sup> Because PET is not stable in ethanol, its partial depolymerization might lead the NF filter to resist more air, simultaneously making it a little nonuniform. However, at this stage of the study, nothing can be claimed. It needs to be investigated further for a possible mechanism of increased pressure drop in the case of ethanol-treated PET.

Breathing comfort is also dependent on rate of moisture transportation through the filter. Breathability test was performed to evaluate WVTR (Figure 5b). It was observed that WVTR of NF filter was superior to that of MB filter.

WF  
99  
97  
75%  
72%  
65% - 95%

} breathability superior

There might be two possible reasons. First, because MB filter has sponge-like structure which resists moisture, it will take longer time to pass through the filter. However, the NF filter has finer structure, uniform morphology, and uniform pore diameter which allow the water vapor to be passed through the filter more efficiently. Second, pressure drop and efficiency tests where NaCl particles were used were done according to ASTM standard, but in the case of WVTR, there was no salt present in water. Because NaCl particle size is larger than pore diameter of NF filters, the pressure drop was recorded higher in the case of the NF filter. However, water vapor has a smaller particle size which can easily pass through both filters. It was also reflected in results of efficiency test that NF filter exhibited consistent efficiency due to uniform pore structure while MB filter's efficiency dropped as a result of ethanol treatment. Concluding performance properties, pressure drop and air permeability were found to be better in the case of MB filter; however breathability results were the opposite. Thus, pressure drop is not a direct indication of breathing comfort or discomfort. As for pressure drop measurement, NaCl particles are used which have larger particle size as compared to that of air, so pressure drop cannot be basis of breathability. WVTR results also confirmed that breathing performance of both types of filters was sufficient for practical use.

Filtration efficiency is one of the major concerns when it comes to face mask performance criteria. Thus, the filtration efficiency test was also performed to investigate the validity of reuse (Figure 4). We found that the filtration efficiency of MB filter significantly dropped to ~84% and ~62% after ethanol spraying with 1 cycle and 10 cycles, respectively (Figure 4a). Similar to spraying treatment, filtration efficiency of MB filter dropped to ~82% after 5 min and ~65% after 24 h ethanol dipping (Figure 4b). Thus, the significant reduction of filtration efficiency of MB filter after ethanol cleaning can lead to a clear conclusion that MB filter which is being used in high rated face masks such as N95 is the best available option for single-use only but is not capable of being reused for face mask applications. Note that we observed disappearing of static surface charge of MB filter after ethanol treatment (Figure 5a). This disappearing of static charge is one of the possible reasons that the filtration efficiency of the MB filter was decreased when treated with ethanol. Actually, it was already known that the filtration efficiency of the MB filter is somehow dependent on the static charge on its surface.<sup>43</sup> We also confirmed that the original NF filter does not have any static charge on its surface. Importantly, the filtration efficiency of the NF filter had a consistent value of around 98% regardless of ethanol treatment type (Figure 4). The maintenance of the filtration efficiency of NF filter might be explained from its filtration mechanism using particle size difference without using static charge.

In addition, we observed that MB filters took more time (about 3 h) to be fully dried, while NF filters were dried quickly within 10 min (data not shown). Considering the recent pandemic, drying time will also be an important factor because some studies reported that MB filter-based N95 mask gives a favorable environment to viruses and bacteria due to its moisture-loving nature.<sup>22</sup>

Besides air permeation and pressure drop, mask filters should possess breathing comfort features for wearers. Thus, transmissions of air, moisture, and carbon dioxide ( $\text{CO}_2$ ) were evaluated using an infrared thermal camera. It was clearly observed that the NF filter exhibited superior breathing

comfort with good thermal behavior to MB filter (Figure 6a). NF filter possesses uniform morphology having fine pore

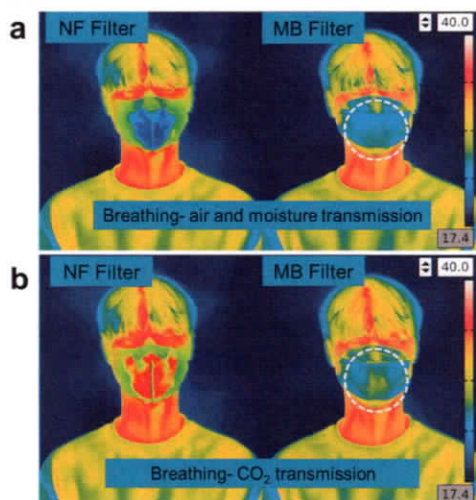


**Figure 6.** Evaluation of breathing comfort by infrared thermal camera: (a) air and moisture transmission and (b)  $\text{CO}_2$  transmission.

diameter (50–100 nm) which is larger than the particle size of air (~4 nm) but smaller than foreign matters including bacteria and viruses (i.e., the particle size of coronavirus is in the range of 80–160 nm).<sup>44</sup> Uniform pore diameter distribution of the NF filter can be one of the possible reasons for good breathing comfort as well as higher and consistent filtration efficiency. In the case of MB filter, diameter distribution was wider due to its nonuniform morphology that can be a possible reason for thermal discomfort and a barrier in the transmission of  $\text{CO}_2$  and foreign matters as well. Figure 6b shows  $\text{CO}_2$  emission mechanism of both types of filters. It can be observed that the MB filter exhibited poor emission as compared to that of NF filter. It can be due to sponge-like structure, higher thickness, and nonuniform pore diameter of MB filter. NF filter is generally thinner and more uniform which allows  $\text{CO}_2$  molecules to pass through quickly.

**Evaluation on the Surface and Morphological Property Changes.** Morphological property changes of both filter types were examined before and after treatment with 75% ethanol (both spraying and dipping treatments). First, through SEM analyses, it was confirmed that there was no significant change in morphology of the NF filter regardless of ethanol treatment (Figure 7a). NF filter had a uniform morphology without any beads formation during the electro-spinning process. The diameter range for all nanofibrous samples was found to be uniform with a narrow diameter distribution. It was interesting to observe that there were no morphological changes of nanofibers even after 24 h dipping time and 10 cycle spraying. In the case of MB filter, nonuniform morphology was clearly observed with a wide range of diameters (Figure 7a). Diameters of MB fibers were found to be from submicrometer to tens of micrometers. Also, there were no alignments in fibers. However, the MB filter was

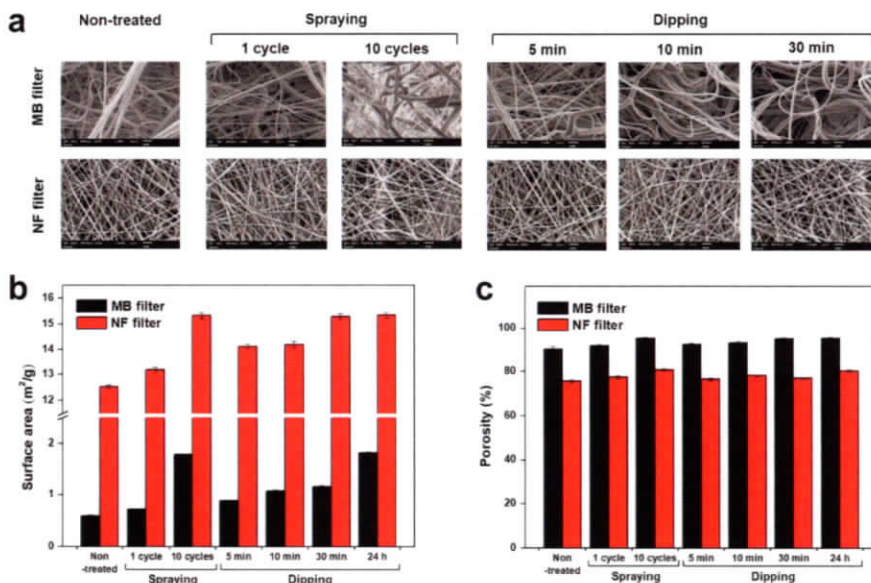


**Figure 7.** (a) SEM images, (b) surface area, and (c) porosity of MB and NF face mask filters before and after spraying and dipping treatments. SEM images were taken at a magnification of 1000 for MB filter and 10 000 for NF filter. The lengths of scale bars are 10  $\mu\text{m}$  for MB filter and 1  $\mu\text{m}$  for NF filter.

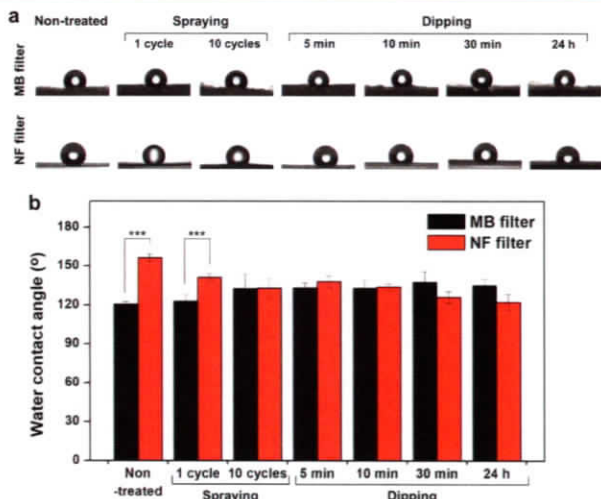


**Figure 8.** (a) Images of water droplets on contacted surfaces and (b) calculated contact angles of MB and NF face mask filters before and after spraying and dipping treatments. The values and error bars represent the mean  $\pm$  standard deviations of at least five samples with statistical significance from unpaired *t* test (\*\*\*( $p < 0.005$ ).

also found to be morphological consistent when treated with ethanol. Magnified SEM images with clear scale bar can be viewed in Supporting Information (Figure S1).

Next, surface area change was analyzed after ethanol treatment. As expected, the MB filter exhibited much lower

surface area (average of  $0.588 \text{ m}^2/\text{g}$ ), while it was increased according to treatment time (Figure 7b); the MB filter with ethanol treatment for 24 h presented a 3-fold higher surface area than the nontreated sample. The same phenomena were also observed for the NF filter. Its high surface area (average of

$12.529 \text{ m}^2 \text{ g}^{-1}$ ) was also increased with increasing treatment time. In the case of MB filter, surface area might increase due to shrinkage of individual fibers on exposure to ethanol (but it was not clearly observed in SEM images; it might be too less to be observed). In the case of the NF filter, the depolymerization of the thinning spun-bond PET layer can be a reason for the increasing trend of surface area. Because this was not the main objective of this study, we do not claim any possible reactions in this work.

Porosities of both types of filters were calculated before and after both types of treatments (Figure 7c). The MB filter exhibited higher porosity (as visually it looked like a sponge) than the NF filter. It was also observed that the porosity of both types of filters displayed an increasing trend with increasing treatment time. Porosities of these filters were also reflected in the results of air permeability and pressure drop.

Hydrophilic or the hydrophobic nature of the filter surface also plays an important role in providing favorable or unfavorable environments to different types of bacteria and viruses.<sup>21</sup> Moisture retaining property is also dependent on the hydrophilic nature of the substrate. Thus, water contact angles of both filters were determined before and after ethanol treatments (Figure 8). It was observed that water contact angles of both filter types were recorded above  $90^\circ$ , indicating that both filters are hydrophobic in nature. In particular, the NF surface had a much larger water contact angle above  $150^\circ$ , which can be considered as a superhydrophobic surface. However, there was a slight increase in the water contact angle of MB filter when treated with ethanol, and it might be due to decreased static surface charge. The water contact angle for the NF filter was slightly decreased after treatment with ethanol due to possible degradation of ester linkages in PET as described in the porosity measurement. Importantly, in any treatment condition, both filters are still in the range of hydrophobicity ( $>90^\circ$ ).<sup>40</sup> Thus, it was considered that the mechanical and chemical properties of both filter materials were not significantly changed by ethanol treatment. The face mask should prevent wetting by moisture and saliva splash to prohibit not only pathogen transmission but also bacterial growth inside.<sup>45,46</sup>

**Evaluation of Antibacterial Efficiency of Ethanol Treatment.** Because ethanol plays an antibiotic role in contaminated microorganisms,<sup>47</sup> antibacterial efficiencies of ethanol treatment process on filters were evaluated. Bacterial cells spread on the filter surface were treated with 75% ethanol and cultured in liquid medium for 12 h. As a result, we found that optical densities of cultured both filters were dramatically decreased when filters were treated with ethanol spraying or dipping process (Figure 9). In particular, spraying with 1 cycle (3 times press) or dipping for 5 min was enough for complete suppression of bacterial growth on both filter types. Thus, it was concluded that simple ethanol treatments are sufficient for an antibacterial effect on both MB and NF filter types.

**Evaluation of Filter Cyocompatibility.** Human keratinocyte HaCaT and endothelial HUVEC cells were selected to consider possible exposure of face mask filter material to face skin and respiratory system.<sup>48,49</sup> As a result, both filter types did not have cytotoxicity to HaCaT cells under all given conditions (Figure 10a). However, in the case of the MB filter, the viability of HUVEC cells was significantly decreased with over 1.5% (w/v) filter extract concentration. According to ISO 10993-5, the relative cell viability above 80% is discriminated to be not cytotoxic at the condition, while the viability within

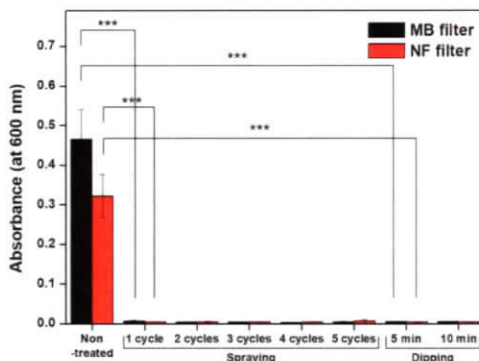


**Figure 9.** Sterilization efficiency of bacterial cells-loaded MB and NF face mask filters before and after spraying and dipping treatments. The samples were incubated in LB media at  $37^\circ\text{C}$  for 12 h, and the remaining cells were quantified by measuring optical density. The values and error bars represent the mean  $\pm$  standard deviations of at least six samples with statistical significance from unpaired *t* test (\*\* $p < 0.005$ ).

80–60% is weak, 60–40% is moderate, and 40–0% is strong cytotoxic.<sup>50</sup> Notably, the NF filter did not have cytotoxicity for both human cell types. These results were also confirmed through live/dead fluorescence microscopic analyses (Figure 10b). Thus, it was concluded that both filters will be harmless to face skin contact while the MB filter might have some toxicity to vascular cells. These might be because the growth condition of the vascular endothelium is more demanding than that of skin keratinocyte.

## CONCLUSIONS

Considering several filter performance parameters, the reusability of the face mask is the need of the hour. Especially, due to the shortage of face masks around the globe in COVID-19 pandemic, it is highly desired to find a way to reuse face mask with minimum chances of risk. Here, we performed a comparative evaluation on the reusability of two types of face mask filters using simple ethanol cleaning method including spraying and dipping. The MB filter exhibited better air permeability (as twice as that of NF filter) before and after treatment by ethanol, and it can be associated with higher porosity of MB filter which was recorded as high as  $\sim 96\%$ . NF filter had lower porosity ( $\lesssim 80\%$ ), and this can also be directly associated with a pressure drop which was higher (up to 183 Pa) before and after treatment with ethanol. Because of good air permeability, pressure drop, and morphological properties regardless of ethanol treatment, both filter types qualify for the basic criteria of face mask application. However, considering the filtration efficiency aspect, while the MB filter will be effective for single use only due to its prompt reduction to  $\sim 64\%$  by ethanol cleaning, the NF filter might be valid for multiple reuses due to its very consistent ( $\sim 97\text{--}99\%$ ) efficiency. In addition, the NF filter did not show cytotoxicity to the tested human cells. Thus, by considering all the comparative evaluations, it can be concluded that while both MB and NF filters have similar filtration performance for single-use applications, the MB filter cannot be reused as its filtration efficiency drops drastically and the NF filter can be

• max. reuses  
to 64% after  
one cleaning

NR stays at  
97% - 99%

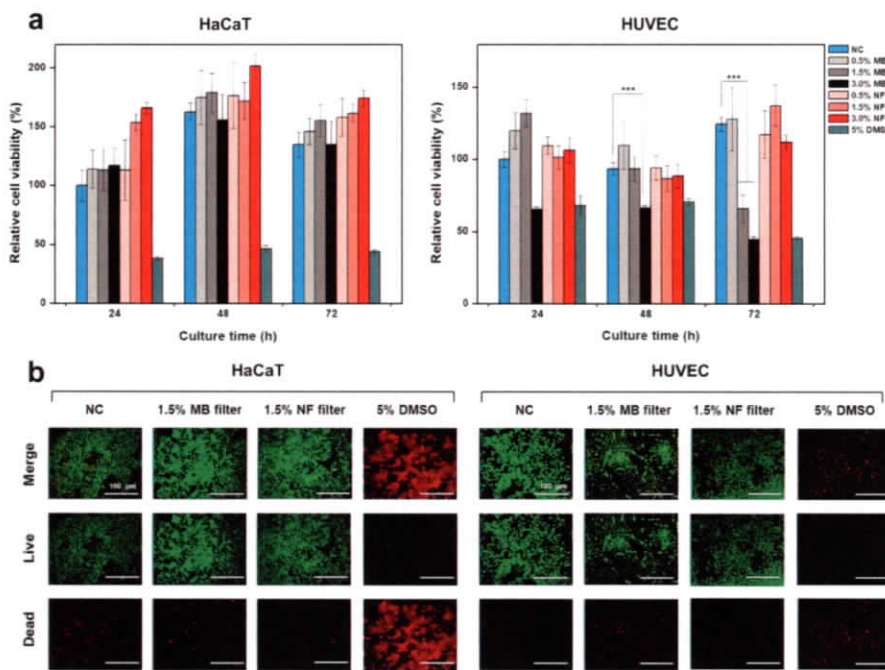


**Figure 10.** Cytocompatibility of MB and NF face mask filters before and after spraying and dipping treatments: (a) relative cell viability of HaCaT and HUVEC cells by CCK-8 assay and (b) live/dead fluorescent cell images at 72 h culture. The length of each scale bar is 100  $\mu\text{m}$ . Blank medium and 5% DMSO were used as negative control (NC) and positive control, respectively. The values and error bars represent the mean  $\pm$  standard deviations of at least five samples with statistical significance from unpaired *t* test (\*\* $p$  < 0.005).

successfully reused multiple times after simple cleaning with ethanol.

## METHODS

**Material Selection and Cleaning Procedures.** Melt blown polypropylene (PP) is often used as filter for face masks. However, polyvinylidene difluoride (PVDF) (electrospun or melt blown) is not commonly used as a filter of mask. We selected PVDF as nanofibrous filter for face mask because of its smoother morphology, uniform pore structure, and good bonding ability with spun bond PET. Although other polymers (PAN, PVA, etc.) can also be used as electrospun nanofibers for filter applications, every polymer has its limitations. Polypropylene (PP) based MB filter (in N95 face mask) was purchased from the market and electrospun polyvinylidene difluoride (PVDF) based NF filter supported by spun bond polyethylene terephthalate (PET) was provided from Lemon Corporation (Gumi, Korea). Composition (w/w) of NF filter was as follows; PET/PVDF = 98:2. MB and NF-based nonwoven filters were cleaned with two types of treatments: spraying of 75% ethanol with 1–10 cycles (1 cycle is 3 times press) and dipping in 75% ethanol for 5 min to 24 h (Figure 1). All samples were air-dried prior to characterization. Then, performance parameters including air permeability, pressure drop, filtration efficiency, and surface and morphological properties were comparatively evaluated.

**Characterization of Performance Parameters.** The filter samples were characterized by scanning electron microscope (SEM; JSM-5300; JEOL Ltd., Japan) to observe the potential change in their structural morphology. Surface area analysis was performed using Brunauer–Emmett–Teller (BET; Tristar II 3020; Shimadzu, Japan). Air permeability analysis was performed using Lab Air IV (FX3300;

area, 38  $\text{cm}^2$  at 125 Pa; TextTest Instruments, Switzerland) to measure airflow rates of the filters. Filtration efficiency analysis was also performed using an automatic filter scanner (AFS153; aerosol, DEHS at 0.3 mm; area, 100  $\text{cm}^2$  at 32LPM; Topas GmbH, Germany) for estimation of reuse time. Differential pressure drop was also investigated using AFS153 (area, 100  $\text{cm}^2$  at 32LPM). An air flow of 32 L/min was opted for air permeability and pressure drop tests, which is standard air flow rate for normal human breathing. Breathing comfort and thermal behavior of wearing face masks were evaluated using an infrared thermal camera (Fotric 226; FOTRIC, China). Breathability test was performed using upright cup method (A-2). Samples were prepared following ASTM E 96.<sup>31</sup> Water vapor transport rate (also used as moisture vapor transport rate MVTR) MVTR was calculated for each specimen.

For measuring porosity, filter mats were cut into 4  $\times$  4  $\text{cm}^2$  of a rectangle shape and subsequently weighed. The filter thickness was measured using a digital thickness gauge at five different places and averaged for further calculations. The apparent volume ( $V_a$ ) was measured using the dimensions of the previously cut filter mat. The volume ( $V_g$ ) was determined by the density of the PET (1.38 g  $\text{cm}^{-3}$ ), PP (0.94 g  $\text{cm}^{-3}$ ), and PVDF (1.78 g  $\text{cm}^{-3}$ ) and their weight ratio in the respective specimen. Porosity was calculated using the following equation:

$$\text{porosity \%} = 1 - \frac{V_g}{V_a} \times 100 \quad (1)$$

For determining the water contact angle, the filter samples were cut into 2  $\times$  7  $\text{cm}^2$  of a rectangle shape. Fully air-dried filters were placed on a microscope slide, and 3  $\mu\text{L}$  of distilled water was dropped on the filter surface through a 23 gauge blunt needle tip. The photograph of

each water droplet on the filter was acquired and analyzed by Smartdrop (Femtobiomed, Korea). The average of the left and right angles was taken as the water contact angle.

**Antibacterial Activity Analyses.** Bacterial dispersion solution was prepared by culturing *Escherichia coli* cells in a liquid medium of 20 g/L Luria–Bertani (LB) broth (Sigma-Aldrich, USA) at 37 °C. The solution was transferred to a spray bottle when its optical density at 600 nm ( $OD_{600}$ ) reached ~1 and sprayed onto filters by pressing 3 times. After ethanol treatment and sufficient air drying, the filters were cut into  $1 \times 1 \text{ cm}^2$  of a rectangle shape and soaked in 0.5 mL of LB medium at 48-well cell culture plates. After 12 h culturing at 37 °C, the  $OD_{600}$  of each medium was measured to configure the survival of the bacterial cells in the filters.

**Cytocompatibility Analyses.** Human keratinocyte (HaCaT) cells and human umbilical vein endothelial (HUVEC; Lonza, Swiss) cells were used for evaluation of cytocompatibility of MB and NF filters. Dulbecco's modified Eagle's medium (DMEM; HyClone) was used for HaCaT cell culture, and EGM-2 BulletKit (Lonza) was used for HUVEC cell culture. Each filter extract was prepared by incubating the filter in the cell culture medium at 37 °C for 24 h according to ISO 10993-5.<sup>50</sup> Precultured cells were seeded in 96-well cell culture plate (SPL Life Science, Korea) to a density of  $1 \times 10^4$  per each well with 100  $\mu\text{L}$  of medium and cultured in a humid incubator with 5% CO<sub>2</sub> at 37 °C. After 24 h, the medium was exchanged with the same amount of medium containing filter extract of 0.5, 1.5, and 3.0% (w/v) and further cultured for 24, 48, and 72 h. Black medium and 5% (v/v) dimethyl sulfoxide (DMSO) were compared as negative and positive controls, respectively. Cell viability was quantitatively determined using the cell counting kit-8 assay (CCK-8; Dojindo, Japan). To visualize cytocompatibility, the cells after 72 h culture were dyed by LIVE/DEAD viability/cytotoxicity kit (Thermo Fisher Scientific, USA). After a 30 min reaction with light-blocking, the sample was observed by a fluorescence microscope (BX60; Olympus, Japan). Calcein-acetoxyethyl ester penetrating into the cytosol of live cells exhibits green light, while ethidium homodimer emits red light penetrating into the nucleus of dead cells. The image was acquired and merged by iSolution (IMT i-Solution Inc., Korea).

## ■ ASSOCIATED CONTENT

### Supporting Information

The Supporting Information is available free of charge at <https://pubs.acs.org/doi/10.1021/acsanm.0c01562>.

SEM images of MB and NF filters ([PDF](#))

## ■ AUTHOR INFORMATION

### Corresponding Authors

Hyung Joon Cha – Department of Chemical Engineering, Pohang University of Science and Technology, Pohang 37673, Korea; [orcid.org/0000-0003-4640-189X](#); Email: [hjcha@postech.ac.kr](mailto:hjcha@postech.ac.kr)

Ick Soo Kim – Nano Fusion Technology Research Group, Institute for Frontier Fibers, Shinshu University, Nagano 386-0017, Japan; [orcid.org/0000-0003-2126-0381](#); Email: [kim@shinshu-u.ac.jp](mailto:kim@shinshu-u.ac.jp)

### Authors

Sana Ullah – Nano Fusion Technology Research Group, Institute for Frontier Fibers, Shinshu University, Nagano 386-0017, Japan

Azeem Ullah – Nano Fusion Technology Research Group, Institute for Frontier Fibers, Shinshu University, Nagano 386-0017, Japan

Jaeyun Lee – Department of Chemical Engineering, Pohang University of Science and Technology, Pohang 37673, Korea

Yeonsu Jeong – Department of Chemical Engineering, Pohang University of Science and Technology, Pohang 37673, Korea

Motahira Hashmi – Nano Fusion Technology Research Group, Institute for Frontier Fibers, Shinshu University, Nagano 386-0017, Japan

Chunhong Zhu – Faculty of Textile Science & Technology, Shinshu University, Nagano 386-0017, Japan; [orcid.org/0000-0001-9251-7899](#)

Kye Il Joo – Department of Chemical Engineering, Pohang University of Science and Technology, Pohang 37673, Korea

Complete contact information is available at:  
<https://pubs.acs.org/10.1021/acsanm.0c01562>

### Author Contributions

<sup>†</sup>S.U., A.U., J.L., and Y.J. have equal contribution in this research. The manuscript was written through contributions of all authors. All authors have given approval to the final version of the manuscript.

### Funding

There was no funding received for this research from any of the funding bodies.

### Notes

The authors declare no competing financial interest.

## ■ ACKNOWLEDGMENTS

We thank Lemon Corporation (Gumi, Korea) for providing NF filter samples and NF filter-based face masks and assistance in testing procedures.

## ■ REFERENCES

- World Health Organization. COVID-19 Global situation. <https://who.sprinklr.com/>.
- Wang, D.; Hu, B.; Hu, C.; Zhu, F.; Liu, X.; Zhang, J.; Wang, B.; Xiang, H.; Cheng, Z.; Xiong, Y.; Zhao, Y.; Li, Y.; Wang, X.; Peng, Z. Clinical Characteristics of 138 Hospitalized Patients with 2019 Novel Coronavirus-Infected Pneumonia in Wuhan, China. *JAMA - J. Am. Med. Assoc.* **2020**, *323* (11), 1061–1069.
- Guan, W.; Ni, Z.; Hu, Y.; Liang, W.; Ou, C.; He, J.; Liu, L.; Shan, H.; Lei, C.; Hui, D. S. C.; Du, B.; Li, L.; Zeng, G.; Yuen, K.-Y.; Chen, R.; Tang, C.; Wang, T.; Chen, P.; Xiang, J.; Li, S.; Wang, J.; Liang, Z.; Peng, Y.; Wei, L.; Liu, Y.; Hu, Y.; Peng, P.; Wang, J.; Liu, J.; Chen, Z.; Li, G.; Zheng, Z.; Qiu, S.; Luo, J.; Ye, C.; Zhu, S.; Zhong, N. Clinical Characteristics of Coronavirus Disease 2019 in China. *N. Engl. J. Med.* **2020**, *382*, 1708–1720.
- Holshue, M. L.; DeBolt, C.; Lindquist, S.; Lofy, K. H.; Wiesman, J.; Bruce, H.; Spitters, C.; Ericson, K.; Wilkerson, S.; Tural, A.; Diaz, G.; Cohn, A.; Fox, L. A.; Patel, A.; Gerber, S. I.; Kim, L.; Tong, S.; Lu, X.; Lindstrom, S.; Pallansch, M. A.; Weldon, W. C.; Biggs, H. M.; Uyeki, T. M.; Pillai, S. K. First Case of 2019 Novel Coronavirus in the United States. *N. Engl. J. Med.* **2020**, *382* (10), 929–936.
- Chan, J. F. W.; Yuan, S.; Kok, K. H.; To, K. K. W.; Chu, H.; Yang, J.; Xing, F.; Liu, J.; Yip, C. C. Y.; Poon, R. W. S.; Tsui, H. W.; Lo, S. K. F.; Chan, K. H.; Poon, V. K. M.; Chan, W. M.; Ip, J. D.; Cai, J. P.; Cheng, V. C. C.; Chen, H.; Hui, C. K. M.; Yuen, K. Y. A Familial Cluster of Pneumonia Associated with the 2019 Novel Coronavirus Indicating Person-to-Person Transmission: A Study of a Family Cluster. *Lancet* **2020**, *395* (10223), 514–523.
- Wax, R. S.; Christian, M. D. Practical Recommendations for Critical Care and Anesthesiology Teams Caring for Novel Coronavirus (2019-NCoV) Patients. *Can. J. Anaesth.* **2020**, *67*, S68.
- Ivanov, D. Predicting the Impacts of Epidemic Outbreaks on Global Supply Chains: A Simulation-Based Analysis on the Coronavirus Outbreak (COVID-19/SARS-CoV-2) Case. *Transp. Res. Part E Logist. Transp. Rev.* **2020**, *136* (March), 101922.
- Kampf, G.; Voss, A.; Scheithauer, S. Inactivation of Coronaviruses by Heat. *J. Hosp. Infect.* **2020**, *105*, 348.

- (9) Chen, N.; Zhou, M.; Dong, X.; Qu, J.; Gong, F.; Han, Y.; Qiu, Y.; Wang, J.; Liu, Y.; Wei, Y.; Xia, J.; Yu, T.; Zhang, X.; Zhang, L. Epidemiological and Clinical Characteristics of 99 Cases of 2019 Novel Coronavirus Pneumonia in Wuhan, China: A Descriptive Study. *Lancet* **2020**, *395* (10223), 507–513.
- (10) Li, Q.; Guan, X.; Wu, P.; Wang, X.; Zhou, L.; Tong, Y.; Ren, R.; Leung, K. S. M.; Lau, E. H. Y.; Wong, J. Y.; Xing, X.; Xiang, N.; Wu, Y.; Li, C.; Chen, Q.; Li, D.; Liu, T.; Zhao, J.; Liu, M.; Tu, W.; Chen, C.; Jin, L.; Yang, R.; Wang, Q.; Zhou, S.; Wang, R.; Liu, H.; Luo, Y.; Liu, Y.; Shao, G.; Li, H.; Tao, Z.; Yang, Y.; Deng, Z.; Liu, B.; Ma, Z.; Zhang, Y.; Shi, G.; Lam, T. T. Y.; Wu, J. T.; Gao, G. F.; Cowling, B. J.; Yang, B.; Leung, G. M.; Feng, Z. Early Transmission Dynamics in Wuhan, China, of Novel Coronavirus-Infected Pneumonia. *N. Engl. J. Med.* **2020**, *382* (13), 1199–1207.
- (11) Zhu, N.; Zhang, D.; Wang, W.; Li, X.; Yang, B.; Song, J.; Zhao, X.; Huang, B.; Shi, W.; Lu, R.; Niu, P.; Zhan, F.; Ma, X.; Wang, D.; Xu, W.; Wu, G.; Gao, G. F.; Tan, W. A Novel Coronavirus from Patients with Pneumonia in China, 2019. *N. Engl. J. Med.* **2020**, *382* (8), 727–733.
- (12) Zhou, P.; Yang, X.-L.; Wang, X. G.; Hu, B.; Zhang, L.; Zhang, W.; Si, H. R.; Zhu, Y.; Li, B.; Huang, C. L.; Chen, H. D.; Chen, J.; Luo, Y.; Guo, H.; Jiang, R. Di; Liu, M. Q.; Chen, Y.; Shen, X. R.; Wang, X.; Zheng, X. S.; Zhao, K.; Chen, Q. J.; Deng, F.; Liu, L. L.; Yan, B.; Zhan, F. X.; Wang, Y.; Xiao, G. F.; Shi, Z. L. A Pneumonia Outbreak Associated with a New Coronavirus of Probable Bat Origin. *Nature* **2020**, *579* (7798), 270–273.
- (13) Li, P.; Fu, J.-B.; Li, K.-F.; Chen, Y.; Wang, H.-L.; Liu, L.-J.; Liu, J.-N.; Zhang, Y.-L.; Liu, S.-L.; Tang, A.; Tong, Z.-D.; Yan, J.-B. Transmission of COVID-19 in the Terminal Stage of Incubation Period: A Familial Cluster. *Int. J. Infect. Dis.* **2020**, *96*, 452.
- (14) Leung, N. H. L.; Chu, D. K. W.; Shiu, E. Y. C.; Chan, K.-H.; McDevitt, J. J.; Hau, B. J. P.; Yen, H.-L.; Li, Y.; Ip, D. K. M.; Peiris, J. S. M.; Seto, W.-H.; Leung, G. M.; Milton, D. K.; Cowling, B. J. Respiratory Virus Shedding in Exhaled Breath and Efficacy of Face Masks. *Nat. Med.* **2020**, *26*, 676–680.
- (15) Wu, H.; Huang, J.; Zhang, C. J. P.; He, Z.; Ming, W.-K. Facemask Shortage and the Novel Coronavirus Disease (COVID-19) Outbreak: Reflections on Public Health Measures. *EClinicalMedicine* **2020**, *21*, 100329.
- (16) Lowe, J. J.; Paladino, K. D.; Farke, J. D.; Boulter, K.; Cawcutt, K.; Emodi, M.; Hankins, R.; Hinkle, L.; Micheels, T.; Schwedhelm, S.; Vasa, A.; Watson, S.; Rupp, M. E. N95 Filtering Facepiece Respirator Ultraviolet Germicidal Irradiation (UVGI) Process for Decontamination and Reuse; Nebraska Medicine, 2020.
- (17) Lee, S.; Cho, A. R.; Park, D.; Kim, J. K.; Han, K. S.; Yoon, I.-J.; Lee, M. H.; Nah, J. Reusable Polybenzimidazole Nanofiber Membrane Filter for Highly Breathable PM2.5 Dust Proof Mask. *ACS Appl. Mater. Interfaces* **2019**, *11* (3), 2750–2757.
- (18) Lin, T. H.; Chen, C. C.; Huang, S. H.; Kuo, C. W.; Lai, C. Y.; Lin, W. Y. Filter Quality of Electret Masks in Filtering 14.6–594 nm Aerosol Particles: Effects of Five Decontamination Methods. *PLoS One* **2017**, *12* (10), e0186217.
- (19) Konda, A.; Prakash, A.; Moss, G. A.; Schmoldt, M.; Grant, G. D.; Guha, S. Aerosol Filtration Efficiency of Common Fabrics Used in Respiratory Cloth Masks. *ACS Nano* **2020**, *14*, 6339.
- (20) Li, Y.; Tokura, H.; Guo, Y. P.; Wong, A. S. W.; Wong, T.; Chung, J.; Newton, E. Effects of Wearing N95 and Surgical Facemasks on Heart Rate, Thermal Stress and Subjective Sensations. *Int. Arch. Occup. Environ. Health* **2005**, *78* (6), 501–509.
- (21) Li, Y.; Wong, T.; Chung, J.; Guo, Y. P.; Hu, J. Y.; Guan, Y. T.; Yao, L.; Song, Q. W.; Newton, E. In Vivo Protective Performance of N95 Respirator and Surgical Facemask. *Am. J. Ind. Med.* **2006**, *49* (12), 1056–1065.
- (22) Balazy, A.; Toivola, M.; Adhikari, A.; Sivasubramani, S. K.; Reponen, T.; Grinshpun, S. A. Do N95 Respirators Provide 95% Protection Level against Airborne Viruses, and How Adequate Are Surgical Masks? *Am. J. Infect. Control* **2006**, *34* (2), 51–57.
- (23) Lim, E. C. H.; Seet, R. C. S.; Lee, K. H.; Wilder-Smith, E. P. V.; Chuah, B. Y. S.; Ong, B. K. C. Headaches and the N95 Face-Mask amongst Healthcare Providers. *Acta Neurol. Scand.* **2006**, *113* (3), 199–202.
- (24) Loeb, M.; Dafoe, N.; Mahony, J.; John, M.; Sarabia, A.; Glavin, V.; Webby, R.; Smieja, M.; Earn, D. J. D.; Chong, S.; Webb, A.; Walter, S. D. Surgical Mask vs N95 Respirator for Preventing Influenza among Health Care Workers: A Randomized Trial. *JAMA - J. Am. Med. Assoc.* **2009**, *302* (17), 1865–1871.
- (25) Kharaghani, D.; Gitigard, P.; Ohtani, H.; Kim, K. O.; Ullah, S.; Saito, Y.; Khan, M. Q.; Kim, I. S. Design and Characterization of Dual Drug Delivery Based on In-Situ Assembled PVA/PAN Core-Shell Nanofibers for Wound Dressing Application. *Sci. Rep.* **2019**, *9* (1), 1–11.
- (26) Ullah, S.; Hashmi, M.; Kharaghani, D.; Khan, M. Q.; Saito, Y.; Yamamoto, T.; Lee, J.; Kim, I. S. Antibacterial Properties of In Situ and Surface Functionalized Impregnation of Silver Sulfadiazine in Polyacrylonitrile Nanofiber Mats. *Int. J. Nanomed.* **2019**, *14*, 2693–2703.
- (27) Hashmi, M.; Ullah, S.; Kim, I. S. Electrospun Momordica Charantia Incorporated Polyvinyl Alcohol (PVA) Nanofibers for Antibacterial Applications. *Mater. Today Commun.* **2020**, *24*, 101161.
- (28) Ullah, A.; Ullah, S.; Khan, M. Q.; Hashmi, M.; Nam, P. D.; Kato, Y.; Tamada, Y.; Kim, I. S. Manuka Honey Incorporated Cellulose Acetate Nanofibrous Mats: Fabrication and in Vitro Evaluation as a Potential Wound Dressing. *Int. J. Biol. Macromol.* **2020**, *155*, 479–489.
- (29) Ullah, S.; Hashmi, M.; Khan, M. Q.; Kharaghani, D.; Saito, Y.; Yamamoto, T.; Kim, I. S. Silver Sulfadiazine Loaded Zein Nanofiber Mats as a Novel Wound Dressing. *RSC Adv.* **2019**, *9* (1), 268–277.
- (30) Khan, M. Q.; Kharaghani, D.; Nishat, N.; Ishikawa, T.; Ullah, S.; Lee, H.; Khatri, Z.; Kim, I. S. The Development of Nanofiber Tubes Based on Nanocomposites of Polyvinylpyrrolidone Incorporated Gold Nanoparticles as Scaffolds for Neuroscience Application in Axons. *Text. Res. J.* **2019**, *89*, 2713.
- (31) Ullah, S.; Hashmi, M.; Hussain, N.; Ullah, A.; Sarwar, M. N.; Saito, Y.; Kim, S. H.; Kim, I. S. Stabilized Nanofibers of Polyvinyl Alcohol (PVA) Crosslinked by Unique Method for Efficient Removal of Heavy Metal Ions. *J. Water Process Eng.* **2020**, *33*, 101111.
- (32) Hashmi, M.; Ullah, S.; Kim, I. S. Copper Oxide (CuO) Loaded Polyacrylonitrile (PAN) Nanofiber Membranes for Antimicrobial Breath Mask Applications. *Curr. Res. Biotechnol.* **2019**, *1* (1), 1–10.
- (33) Chen, Y.; Amiri, A.; Boyd, J. G.; Naraghi, M. Promising Trade-Off Between Energy Storage and Load Bearing in Carbon Nanofibers as Structural Energy Storage Devices. *Adv. Funct. Mater.* **2019**, *29* (33), 1901425.
- (34) Morent, R.; De Geyter, N.; Leyts, C.; Gengembre, L.; Payen, E. Comparison between XPS- And FTIR-Analysis of Plasma-Treated Polypropylene Film Surfaces. *Surf. Interface Anal.* **2008**, *40* (3–4), 597–600.
- (35) Shen, Y.; Wu, P. Two-Dimensional ATR-FTIR Spectroscopic Investigation on Water Diffusion in Polypropylene Film: Water Bending Vibration. *J. Phys. Chem. B* **2003**, *107* (18), 4224–4226.
- (36) Liu, X. D.; Sheng, D. K.; Gao, X. M.; Li, T. B.; Yang, Y. M. UV-Assisted Surface Modification of PET Fiber for Adhesion Improvement. *Appl. Surf. Sci.* **2013**, *264*, 61–69.
- (37) Wei, Y.; Chu, H. Q.; Dong, B. Z.; Li, X.; Xia, S. J.; Qiang, Z. M. Effect of TiO<sub>2</sub> Nanowire Addition on PVDF Ultrafiltration Membrane Performance. *Desalination* **2011**, *272* (1–3), 90–97.
- (38) Madaeni, S. S.; Zinadini, S.; Vatanpour, V. A New Approach to Improve Antifouling Property of PVDF Membrane Using in Situ Polymerization of PAA Functionalized TiO<sub>2</sub> Nanoparticles. *J. Membr. Sci.* **2011**, *380* (1–2), 155–162.
- (39) Rahimpour, A.; Jahanshahi, M.; Rajaeian, B.; Rahimnejad, M. TiO<sub>2</sub> Entrapped Nano-Composite PVDF/SPEs Membranes: Preparation, Characterization, Antifouling and Antibacterial Properties. *Desalination* **2011**, *278* (1–3), 343–353.
- (40) De Castro, R. E. N.; Vidotti, G. J.; Rubira, A. F.; Muniz, E. C. Depolymerization of Poly(Ethylene Terephthalate) Wastes Using Ethanol and Ethanol/Water in Supercritical Conditions. *J. Appl. Polym. Sci.* **2006**, *101* (3), 2009–2016.

- (41) Fernandes, J. R.; Amaro, L. P.; Muniz, E. C.; Favaro, S. L.; Radovanovic, E. PET Depolymerization in Supercritical Ethanol Conditions Catalysed by Nanoparticles of Metal Oxides. *J. Supercrit. Fluids* **2020**, *158*, 104715.
- (42) Kim, J.-H.; Roberge, R. J.; Powell, J. B.; Shaffer, R. E.; Ylitalo, C. M.; Sebastian, J. M. Pressure Drop of Filtering Facepiece Respirators: How Low Should We Go? *Int. J. Occup. Med. Environ. Health* **2015**, *28* (1), 71–80.
- (43) Kılıç, A.; Shim, E.; Pourdeyhimi, B. Electrostatic Capture Efficiency Enhancement of Polypropylene Electret Filters with Barium Titanate. *Aerosol Sci. Technol.* **2015**, *49* (8), 666–673.
- (44) Guy, J. S.; Breslin, J. J.; Breuhaus, B.; Vivrette, S.; Smith, L. G. Characterization of a Coronavirus Isolated from a Diarrheic Foal. *J. Clin. Microbiol.* **2000**, *38* (12), 4523–4526.
- (45) Wang, N.; Cai, M.; Yang, X.; Yang, Y. Electret Nanofibrous Membrane with Enhanced Filtration Performance and Wearing Comfortability for Face Mask. *J. Colloid Interface Sci.* **2018**, *530*, 695–703.
- (46) Ekabutr, P.; Chuysinuan, P.; Suksamrarn, S.; Sukhumsirichart, W.; Hongmanee, P.; Supaphol, P. Development of Antituberculosis Melt-Blown Polypropylene Filters Coated with Mangosteen Extracts for Medical Face Mask Applications. *Polym. Bull.* **2019**, *76* (4), 1985–2004.
- (47) Yoo, J.-H. Review of Disinfection and Sterilization – Back to the Basics. *Infect. Chemother.* **2018**, *50* (2), 101.
- (48) Cao, Y.; Gong, Y.; Liu, L.; Zhou, Y.; Fang, X.; Zhang, C.; Li, Y.; Li, J. The Use of Human Umbilical Vein Endothelial Cells (HUVECs) as an In Vitro Model to Assess the Toxicity of Nanoparticles to Endothelium: A Review. *J. Appl. Toxicol.* **2017**, *37* (12), 1359–1369.
- (49) López-García, J.; Lehocký, M.; Humpolíček, P.; Sáha, P. HaCaT Keratinocytes Response on Antimicrobial Atelocollagen Substrates: Extent of Cytotoxicity, Cell Viability and Proliferation. *J. Funct. Biomater.* **2014**, *5* (2), 43–57.
- (50) ISO 10993-5:2009 Biological Evaluation of Medical Devices. Part 5: Tests for In Vitro Cytotoxicity; International Organization for Standardization: Geneva, Switzerland.
- (51) ASTM E96 Standard Test Methods for Water Vapor Transmission of Shipping Containers; ASTM, 2003; Vol. 95 (Reapproved), pp 4–6.